

Two-photon assisted clock comparison to picosecond precision

Shi-Wei Zhang (张世伟)^{1,2,3}, Jia-Zheng Song (宋家争)^{1,3},
Yin-Ping Yao (姚银萍)¹, Ren-Gang Wan (万仁刚)¹ and Tong-Yi
Zhang (张同意)¹

¹ State Key Laboratory of Transient Optics and Photonics, Xi'an Institute of Optics and Precision Mechanics, Chinese Academy of Science, Xi'an 710119, China

² School of Science, Xi'an Jiaotong University, Xi'an 710049, China

³ University of Chinese Academy of Sciences, Beijing 100049, China

E-mail: zsw@opt.ac.cn

Abstract. We have experimentally demonstrated a clock comparison scheme utilizing time-correlated photon pairs generated from the spontaneous parametric down conversion process of a laser pumped beta-barium borate crystal. The coincidence of two-photon events are analyzed by the cross correlation of the two time stamp sequences. Combining the coarse and fine part of the time differences at different resolutions, a 64 ps precision for clock synchronization has been realized. We also investigate the effects of hardware devices used in the system on the precision of clock comparison. The results indicate that the detector's time jitter and the background noise will degrade the system performance. With this method, comparison and synchronization of two remote clocks could be implemented with a precision at the level of a few tens of picoseconds.

PACS numbers: 06.30.Ft, 42.50.Ex, 42.65.Lm

Keywords: clocks comparison, cross correlation, coincidence measurement, time-correlated photon pairs

1. Introduction

High accurate clocks comparison and synchronization are important for fundamental physics research and practical applications, such as, Global Navigation Satellite Systems (GNSSs), power transmission grid, telecommunication, distributed network, etc. There are several modern protocols to synchronize remote clocks, such as network time protocol (NTP), precision time protocol (PTP), and GNSSs [1]. NTP is a method to synchronize clocks by means of message passing over the internet. Its nominal accuracy is in the low tens of milliseconds on wide area networks to sub-milliseconds on a local area network. For the PTP described in IEEE 1588 [2], it is possible to synchronize distributed clocks with an accuracy of less than 1 microsecond via Ethernet networks. In the widely used GNSS scheme, the two-way satellite time and frequency transfer method [3], which takes advantage of exchanging modulated signals between two sites to cancel most effects that impact on the accuracy, is at the level of one nanosecond [3, 4].

Recently, some new methods both in theory and experiment have been reported to improve the accuracy of remote clock synchronization to the level of few picoseconds. One is the time transfer through optical fibers, which can reach the accuracy of 100 ps due to the wider bandwidth of the transmission [5, 6, 7, 8, 9]. Another way is the time transfer by laser link (T2L2), by using the propagation of light pulses between satellite and ground clocks or between remote clocks on the earth [10]. The expected performance of T2L2 is in the 100 ps range for accuracy, with an ultimate time stability about 1 ps over 1,000 s and 10 ps over 1 day [11, 12]. With the help of quantum entanglement, several quantum clock synchronization schemes have been proposed in theory [13, 14, 15, 16], they provide a new way to synchronize remote clocks, and the accuracy can even reach a level of the standard quantum limit. Experimental demonstration of quantum clock synchronization using entangled photon pairs has been carried out by Valencia et al. [17]. This method relied on the measurement of the second-order time-correlation function of entangled photons, and can achieve a resolution of picoseconds. Ho et al. provided an algorithm to detect the time and frequency differences of independent clocks based on the remote coincidence identification of time-correlated photon pairs [18]. Using the algorithm, remote clocks can be synchronized without dedicated coincidence hardware or very stable reference clocks with nanosecond precision.

In this paper, we present a remote clock comparison experiment using time-correlated photon pairs generated from the spontaneous parametric down conversion (SPDC) process of a laser pumped beta-barium borate (BBO) crystal. Using the cross correlation method, we have identified the time-correlated photon pairs events that detected by two remote clocks. The time difference of the two clocks is obtained via the cross correlation and peak searching process at a 64 ps resolution, and the standard deviation of the time difference is 55.92 ps. This scheme can be used in quantum communication and quantum position systems to improve the precision of clock synchronization.

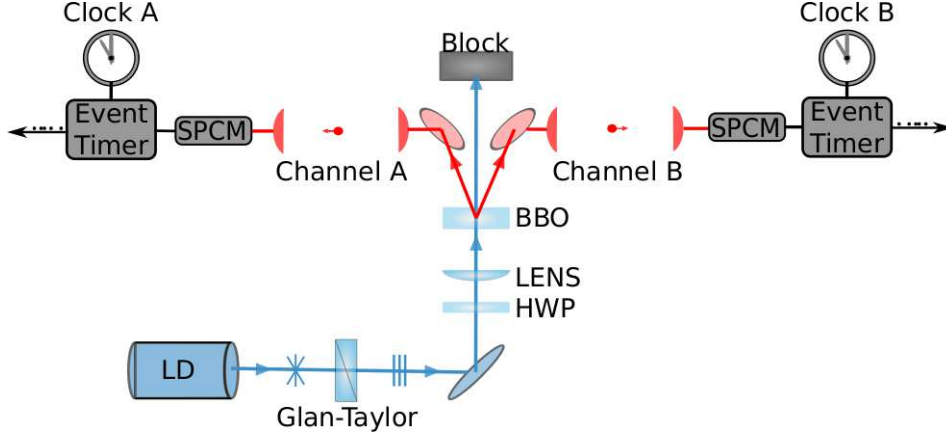


Figure 1. The experimental setup of remote clocks comparison scheme.

2. Cross correlation method for clock comparison

The process of comparing remote clocks with time-correlated photon pairs is similar to the problem of time delay estimation [19, 20]. The arrival times of single photons are recorded as time stamps, and it can be mathematically modeled as,

$$A(t) = s_1(t) + n_1(t) \quad (1a)$$

$$B(t) = s_2(t) + n_2(t) \quad (1b)$$

where $s_{1,2}(t)$ are the arrival time sequences of the photons to detectors, and $n_{1,2}(t)$ represent the erroneous time stamps caused by detector's dark counts and background light. The signals $s_{1,2}$ are assumed to be uncorrelated with noises $n_{1,2}$, and the noises $n_{1,2}$ are also uncorrelated with each other.

For the comparison of two remote clocks, we calculate the cross correlation of two time sequences $A(t)$ and $B(t)$. By a linear searching process, the time difference of clocks can be found in the peak position of cross correlation function, i.e.

$$T_{diff} = \arg \max_t [R_c(t)] \quad (2)$$

where R_c is the cross correlation of $A(t)$ and $B(t)$, and can be calculated via fast Fourier transformations (FFT) and their inverse [18],

$$R_c = E[A(t)B(t)] = \mathcal{F}^{-1}[\mathcal{F}^*[A] \cdot \mathcal{F}[B]] \quad (3)$$

where E denotes the expectation; \mathcal{F} , \mathcal{F}^{-1} represent FFT and its inverse; superscript $*$ indicates complex conjugate operation.

3. Clock comparison experiment

3.1. Experimental setup

The schematic of the clock comparison experiment is given in figure 1. A 403 nm laser diode with 30 mW power impinges on a type-II non-collinear cutting 2 mm long

BBO crystal to generate two down-converted photons with degenerated wavelength centered at 806 nm. The two single photons are then distributed via channel A and channel B to two remote sites, where there are two clocks (clock A and clock B) need to be synchronized. After flying in free space and collected by optical systems, single photons are detected by Si avalanche photo diodes (PerkinElmer SPCM-AQRH-16) with response-time jitter about 350 ps [21]. The arrival times of single photons at the detectors are recorded by two event timers (A033-ET). The event timer is connected with a rubidium clock (SRS 625 with the frequency stability 3.16×10^{-11} in 10 seconds) and locked to the rubidium clock's 10 MHz oscillator. When the detector receives a single photon, the event timer generates an output signal of the arrival time of the single photon. So, during the acquisition time, we get two sequences of arrival time stamps $\{A(t)\}$ and $\{B(t)\}$.

To characterize the time-correlation of down-converted photons, we employ the hardware coincidence method to measure the coincidence time distribution. In this method, the hardware coincidence equipment consists of a nanosecond delay (ORTEC 425A), a time-to-amplitude converter (TAC), and a multi-channel analyzer (MCA). One of the output signal from the two single photon detectors is used as the start signal of TAC, and the other one as the stop signal after passing through a nanosecond delay, the coincidence time distribution of the two-photon is recorded in MCA by measuring the pulse height distribution of the output of TAC. The result is shown in figure 2, in which the time axis represents the relative delay of two photons, the full-width at half-maximum of the coincidence time distribution peak is 0.698 ns. It's a combine effect of detector jitter, electric delay in TAC, and the bin size of MCA, but mainly due to the detector's response-time jitter. A bandpass interference filter with 3 nm bandwidth and 50% transmissivity is used to block the background light. During a 10 seconds sampling period, 4207 coincidence counts are recorded. The average coincidence detection rate is about 420 counts per second to ensure that there are sufficient number of two-photon events to find the time difference of remote clocks.

3.2. Time difference calculation

Generally, the common method for finding the time difference is to calculate the cross correlation of two signals and to select the peak of in cross correlation result as the estimate of the time difference T_{diff} .

In the clock comparison process, if we directly calculate the cross correlation, the size of FFT arrays will exceed 10^{10} (for time resolution of 10 ps and 0.1 s acquisition time). It's a time-consuming process and also impractical. To solve this problem, we use the method proposed by Ho et al. [18], to calculate the coarse and fine parts of T_{diff} separately in a moderate size. Then, combining the results of the two parts, a high resolution result can be obtained. In this method, the time stamp sequences are converted into discrete arrays with a time resolution δt ,

$$A_k = \sum_i \delta_{k, \lfloor (t_i / \delta t) \bmod N \rfloor} \quad k = 0, \dots, N - 1 \quad (4)$$

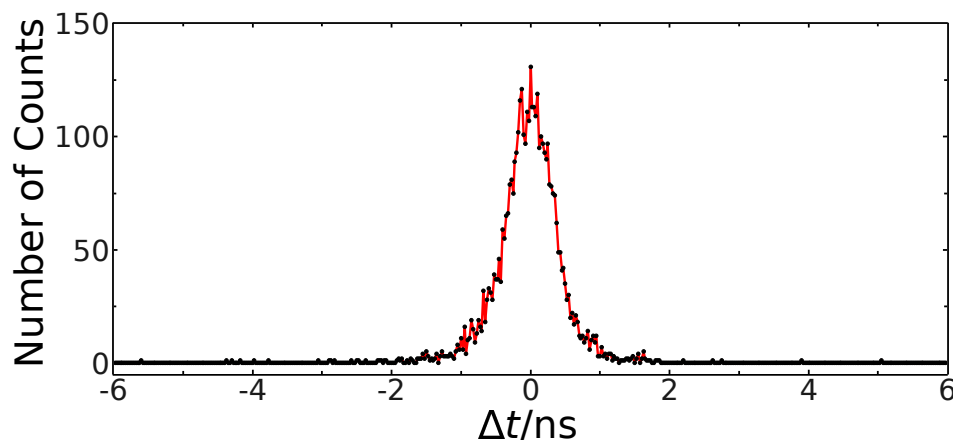


Figure 2. The coincidence time distribution of two-photon. The horizontal axis Δt represents the relative delay of two single photons, and the vertical axis is the number of coincidence counts in corresponding relative delay.

where N is the size of discrete arrays, and the same for B_k . Then, substitute A_k and B_k into the equations (2) and (3), we can obtain the peak position corresponding to a resolution δt and modulo $N\delta t$.

The time difference of two time stamp sequences may be very long that a large size of the discrete array is needed. In practice, we adjust the two sequences and make them align left. Firstly, the difference of the first time stamps of each sequence, named as ΔT_1 , is calculated by a subtract operation. Based on ΔT_1 , the two sequences are adjusted to make the first element of each sequence identical. Then, the relative offset of two revised sequences ΔT_2 is calculated by the cross correlation method. Finally, by simply adding the relative offset ΔT_2 to the first time stamp difference ΔT_1 , the time difference of two time stamp sequences can be expressed as $\Delta T = \Delta T_1 + \Delta T_2$.

In the cross correlation calculation, the noise events may lead to a high background which seriously smooth the correlation peak. In the worse case, it maybe give a false result. Generally, the noise events can be remit by using the prefilter method in generalized correlator [22]. We use a simple method to get rid of the obvious noise events. At first, check the adjacent time stamps, if they are from the same detector, then drop the previous one and compare with the next one, continue until the adjacent events are from different detectors. Secondly, set a threshold Δt_{th} , and remove the adjacent pairs with time difference exceed the threshold. With this method, most of the obvious uncorrelated events can be eliminated and only the events with the most probability to be similar to the true two-photon pairs maintained.

3.3. Clock comparison result

For a efficiently cross correlation calculation, we define the size of cross correlation array $N = 2^{23}$, and set the coarse resolution as 2^{15} ps. The corresponding acquisition

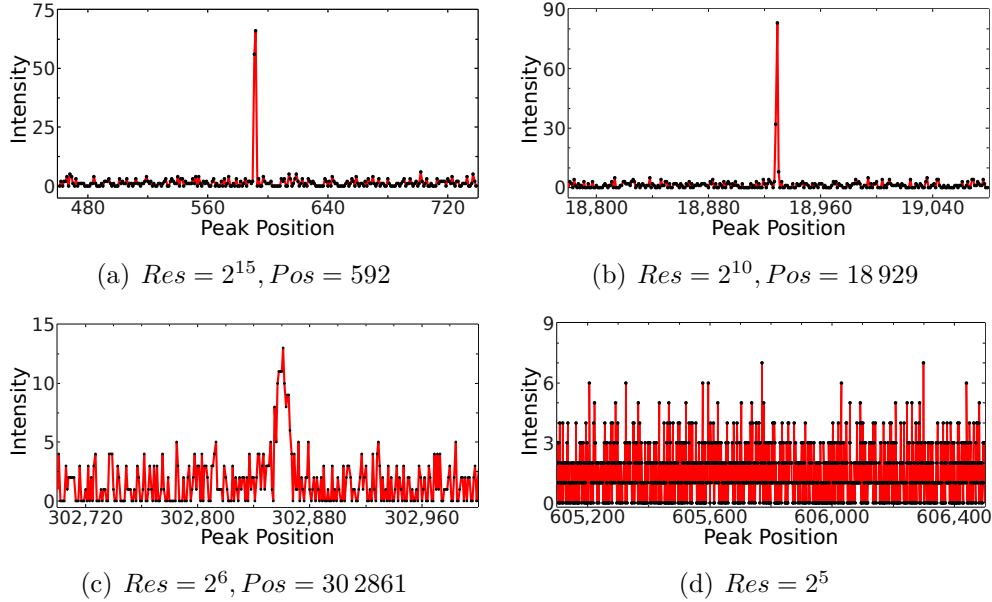


Figure 3. The cross correlation results of two revised sequences at different resolutions. Res represents the resolution, and Pos indicates the peak position in the array.

time is 2^{38} ps to make sure that there are enough photon pairs events in the subset of the time stamp sequence. One subset is extracted during the acquisition time and there are 3097 time stamps from sequence A, and 4094 from sequence B. The first time stamps difference ΔT_1 of the two subset sequences is 1716 789 048 793 ps. Then, the two sequences are revised, and the relative offset ΔT_2 is calculated using the method in section 3.2 with different resolutions in 2^{15} ps, 2^{10} ps, 2^6 ps, and 2^5 ps, respectively.

The cross correlation results of the two revised sequences are show in figure 3. The peaks in figure 3(a) at resolution 2^{15} ps, figure 3(b) at resolution 2^{10} ps, and figure 3(c) at resolution 2^6 ps are sharp enough to be identified with sufficient significance. Consider the situation at resolution 2^5 ps or below, as shown in figure 3(d), it's hard to uniquely identify an obvious signal peak. In such case, the cross correlation of the two-photon events is submerged in noise that mainly caused by the jitter of detectors and the background light.

The clock comparison results of the selected subset time stamp sequences are shown in table 1. The time difference at the coarse resolution 2^{15} ps is directly calculated and a 1716 808 447 449 ps difference is obtained. The time differences at fine resolutions 2^{10} ps and 2^6 ps are calculated by combining the least significant byte of the fine results with the most significant byte of the coarse result that calculated at 2^{15} ps resolution, respectively. Finally, the time difference at 2^{10} ps resolution is 1716 808 432 089 ps and 1716 808 431 897 ps for the resolution at 2^6 ps.

We successively extract 20 subsets, with the same acquisition time 2^{38} ps, from the time stamp sequences of $\{A(t)\}$ and $\{B(t)\}$. The time difference of each subset

Table 1. The clock comparison results of one subset at different resolutions.

ΔT_1 [ps]	1716 789 048 793		
Res [ps]	2^{15}	2^{10}	2^6
Pos	592	18 929	302 861
ΔT [ps]	1716 808 447 449	1716 808 432 089	1716 808 431 897

Table 2. The clock comparison results of 20 subsets at resolution 2^6 ps.

M^a	ΔT^b [ps]	M^a	ΔT^b [ps]
1	1716 808 431 897	11	1716 808 431 939
2	1716 808 431 950	12	1716 808 431 935
3	1716 808 431 978	13	1716 808 431 919
4	1716 808 431 868	14	1716 808 431 918
5	1716 808 432 016	15	1716 808 431 848
6	1716 808 431 938	16	1716 808 431 825
7	1716 808 431 928	17	1716 808 431 873
8	1716 808 431 896	18	1716 808 431 849
9	1716 808 431 965	19	1716 808 431 807
10	1716 808 431 964	20	1716 808 431 843

^a The column number indicates the M th subset.^b ΔT is the time difference corresponding to each subset sequences.

is calculated at the resolution 2^6 ps, as shown in table 2. The mean value of the time differences is $\overline{\Delta T} = 1/M \sum_{i=1}^M \Delta T_i = 1716\,808\,431\,907\,ps$, and the standard deviation is calculate by

$$\sigma = \left[\sum_{i=1}^M (\Delta T_i - \overline{\Delta T})^2 / (M - 1) \right]^{1/2} = 55.92\,ps. \quad (5)$$

Finally, the time difference between two remote clocks is estimated to be $1716\,808\,431\,907 \pm 56\,ps$.

4. System performance analysis

To analyze the effects of hardware devices, such as the rubidium clocks, event timers, and single photon detectors on the precision of clock synchronization system, we propose four different schemes, named as scheme I-IV shown in figure 4. In schemes I-III, two square pulse signals with 1MHz frequency and 2% duty (the pulse width is 20 ns, just for simulating the output electric pulse of the single photon detector) from a signal generator are used as the input signals of the clock comparison system. In scheme I, two input signals connect with the two channels of one event timer, and the event timer connects with a clock; for scheme II, each input signal connects with an event timer, two event timers connect with the same clock; and in scheme III, each input signal connects with an event timer, but the two event timers connect with different clocks; the scheme

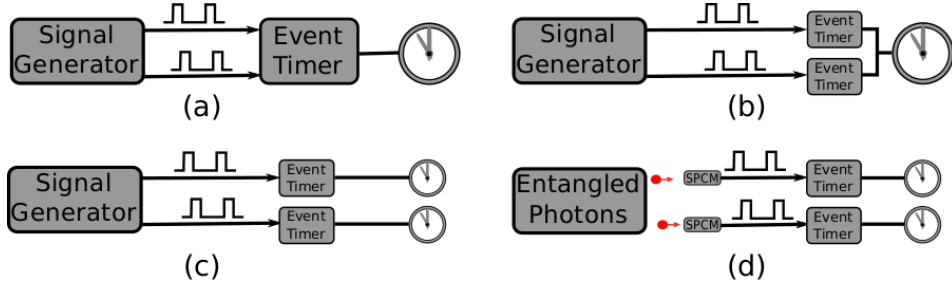


Figure 4. Sketch of the schemes I-IV. (a), (b), (c), and (d) correspond to the schemes I-IV in sequence.

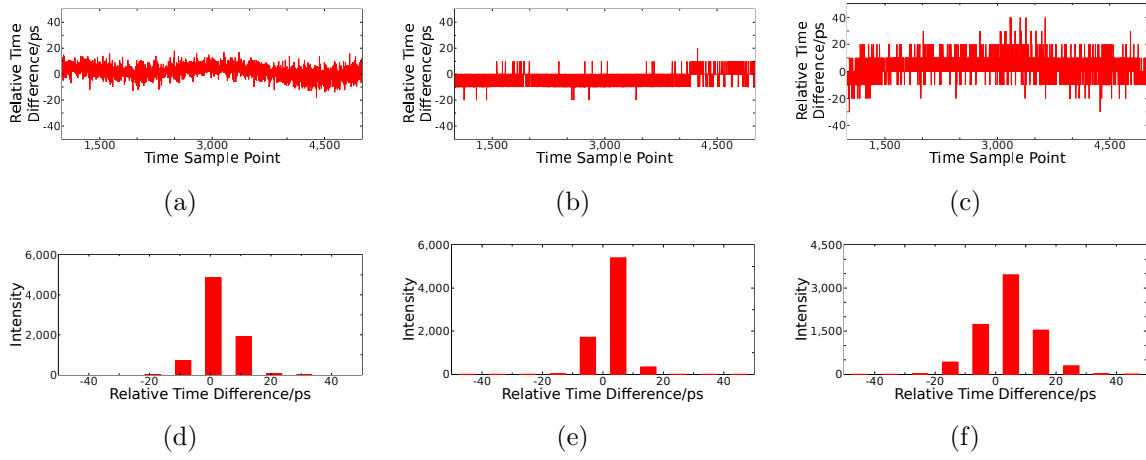


Figure 5. Statistical results for the relative time difference of two time stamp sequences $\{A'(t)\}$ and $\{B'(t)\}$. Figure 5(a), figure 5(b) and figure 5(c) illustrate the relative time difference distribution for part of the time sequences. Figure 5(d), figure 5(e) and figure 5(f) are the histograms of the relative time difference. Figure 5(a) and figure 5(d) in the first column are the results for scheme I, the second and the third columns are the results for scheme II and scheme III, respectively.

in section 3 is defined as scheme IV, which is the same as scheme III except that the two input signals are generated from two single photon detectors.

In the schemes I-III, two time stamp sequences are recorded as $\{A'(t)\}$ and $\{B'(t)\}$, and each sequence contains 7500 time stamps. The relative time difference of two sequences $\{A'(t)\}$ and $\{B'(t)\}$ can be directly obtain by a subtraction operation. The standard deviation of the relative time difference is calculated to character the performance of system. By comparing different schemes, the effects of system components can be analyzed individually.

At first, the influence of event timers is analyzed by comparing scheme I with scheme II. We ignore the difference in the two channels of one event timer. The only difference in these two schemes is the event timer. The standard deviation of the relative time difference of two input signals in scheme I is $\sigma_1 = 5.15$ ps, the distribution and the histogram of the relative time difference in scheme I is shown in figure 5(a) and

figure 5(d). The result for scheme II is that $\sigma_2 = 4.67$ ps, and the statistical results are shown in figure 5(b) and figure 5(e). For event timers, the standard deviations of total error in measurement of time intervals between events are calibrated as $\sigma_{ET1} = 2.91$ ps, $\sigma_{ET2} = 3.01$ ps. So, we can see that there is no obvious difference in the results of scheme I and scheme II, σ_1 and σ_2 are almost the same. Therefore, the effect of event timers on the precision of clock comparison can be ignored when different equipments are used in remote sites.

Secondly, the effect of clock's frequency offset is investigated by comparing scheme II and scheme III. If the two clocks used in experiments have exactly the same frequency, i.e. $\delta u = 0$, then the contribution of two-photon events will all end up in a single time bin in the cross correlation calculation. While for the case $\delta u \neq 0$, the correlated events will spread out, and the arrival time stamps of the single photon streams become $t'_i = t_i \times (1 + \delta u)$. This can not only reduce the intensity of the cross correlation peak, but also increase the width of the peak. In scheme II the two event timer are connected to the same atomic clock, which corresponds to the case that two clocks with no frequency offset. While in scheme III the two event timer are connected to different atomic clocks, and there may exist some frequency offset. For scheme III, the standard deviation of the measured relative time difference is $\sigma_3 = 8.99$ ps, and the statistical results are shown in figure 5(c) and figure 5(f). Compared with the results in scheme II, σ_3 is larger than σ_2 . It means that the offset in clock frequency will decrease the precision of the clock comparison. As the frequency stability of rubidium clock is 3.16×10^{-11} , the time drift during the acquisition time ($2^{38} \text{ ps} \approx 0.275 \text{ s}$) is about 8.69 ps. Thus for the 64 ps resolution, i.e. a 64 ps coincidence window for time-correlated photon pair events, the time drift caused by frequency offset could not affect the cross correlation result. Only in the cases that the resolution is comparable to the time drift or even small (i.e. time resolution less than 8.69 ps), the effects of the time drift caused by frequency offset on clock comparison need to be considered.

Finally, the effect of single photon detector's time jitter is studied by comparing scheme IV with scheme III. The difference of the two schemes is that the signal from single photon detector has a random time jitter along with background noise. Similar to the mechanism that the clock's frequency offset affects the cross correlation, the detector's time jitter leads to a random fluctuation of the single photon's arrival time. As shown in section 3.3, the standard deviation of the time differences in scheme IV at 64 ps resolution is $\sigma = 55.92$ ps, whereas in scheme III $\sigma_3 = 8.99$ ps. Therefore, the detector's time jitter and the background noise seriously degrade the accuracy of the clock comparison.

5. Conclusion

In conclusion, a 64 ps precision for clock comparison has been realized using the time-correlated two-photon pairs. The time difference of two remote clocks is calculated by cross correlation method and the peak searching process after eliminating the

obvious noise events. The influences of the event timer, the clock's frequency offset, and the single photon detector's time jitter are analyzed by comparing four schemes with different hardware devices in the clock comparison system. The results show that the main influence is the detector's time jitter and background noise, the clock's frequency offset may degrade the performance of system depending on the coincidence window, and the effect of event timer can be ignored. In addition, as we know that a 67 km fiber-optical quantum key distribution system [23] and a 144 km free space transmission of entangled photon pairs have been realized in experiments [24, 25], combining the two-photon assisted clock comparison scheme with the technologies in quantum communication, high precision synchronization between long distance separated clocks could be realized in future.

Acknowledgments

This work was supported by the National Natural Science Foundation of China under Grant Nos. 61475191, 61176084, and 11174282; and the Open Research Fund of Key Laboratory of Spectral Imaging Technology, Chinese Academy of Sciences.

References

- [1] J.C. Eidson. *Measurement, Control, and Communication Using IEEE 1588*. Advances in Industrial Control. Springer, 2006.
- [2] IEEE standard for a precision clock synchronization protocol for networked measurement and control systems. *IEEE Std 1588-2008 (Revision of IEEE Std 1588-2002)*, pages c1–269, July 2008.
- [3] D. Piester, A. Bauch, L. Breakiron, D. Matsakis, B. Blanzano, and O. Koudelka. Time transfer with nanosecond accuracy for the realization of international atomic time. *Metrologia*, 45(2):185, 2008.
- [4] H. Esteban, J. Palacio, F. Galindo, T. Feldmann, A. Bauch, and D. Piester. Improved GPS-based time link calibration involving ROA and PTB. *Ultrasonics, Ferroelectrics, and Frequency Control, IEEE Transactions on*, 57(3):714–720, March 2010.
- [5] M. Rost, M. Fujieda, and D. Piester. Time transfer through optical fibers (TTTOF): Progress on calibrated clock comparisons. In *EFTF-2010 24th European Frequency and Time Forum*, pages 1–8, April 2010.
- [6] V. Smotlacha, A. Kuna, and W. Mache. Time transfer using fiber links. In *EFTF-2010 24th European Frequency and Time Forum*, pages 1–8, April 2010.
- [7] Łukasz Śliwczyński, Przemysław Krehlik, and Marcin Lipiński. Optical fibers in time and frequency transfer. *Measurement Science and Technology*, 21(7):075302, 2010.
- [8] D. Piester, M. Rost, M. Fujieda, T. Feldmann, and A. Bauch. Remote atomic clock synchronization via satellites and optical fibers. *Advances in Radio Science*, 9:1–7, 2011.
- [9] M Rost, D Piester, W Yang, T Feldmann, T Wübbena, and A Bauch. Time transfer through optical fibres over a distance of 73 km with an uncertainty below 100 ps. *Metrologia*, 49(6):772, 2012.
- [10] E Samain and P Fridelance. Time transfer by laser link (T2L2) experiment on mir. *Metrologia*, 35(3):151, 1998.
- [11] P. Guillemot, K. Gasc, I. Petitbon, E. Samain, P. Vrancken, J. Weick, D. Albanese, F. Para, and

- J.-M. Torre. Time transfer by laser link: The T2L2 experiment on Jason 2. In *International Frequency Control Symposium and Exposition, 2006 IEEE*, pages 771–778, June 2006.
- [12] E. Samain, P. Exertier, P. Guillemot, F. Pierron, D. Albanese, J. Paris, J. Torre, and S. Leon. Time transfer by laser link - T2L2: Current status of the validation program. In *EFTF-2010 24th European Frequency and Time Forum*, pages 1–8, April 2010.
- [13] Isaac Chuang. Quantum algorithm for distributed clock synchronization. *Phys. Rev. Lett.*, 85:2006–2009, Aug 2000.
- [14] Richard Jozsa, Daniel Abrams, Jonathan Dowling, and Colin Williams. Quantum clock synchronization based on shared prior entanglement. *Phys. Rev. Lett.*, 85:2010–2013, Aug 2000.
- [15] Vittorio Giovannetti, Seth Lloyd, and Lorenzo Maccone. Positioning and clock synchronization through entanglement. *Phys. Rev. A*, 65:022309, Jan 2002.
- [16] Mark de Burgh and Stephen Bartlett. Quantum methods for clock synchronization: Beating the standard quantum limit without entanglement. *Phys. Rev. A*, 72:042301, Oct 2005.
- [17] Alejandra Valencia, Giuliano Scarcelli, and Yanhua Shih. Distant clock synchronization using entangled photon pairs. *Applied Physics Letters*, 85(13):2655–2657, 2004.
- [18] Caleb Ho, Antía Lamas-Linares, and Christian Kurtsiefer. Clock synchronization by remote detection of correlated photon pairs. *New Journal of Physics*, 11(4):045011, 2009.
- [19] C. Knapp and G. Clifford Carter. The generalized correlation method for estimation of time delay. *Acoustics, Speech and Signal Processing, IEEE Transactions on*, 24(4):320–327, Aug 1976.
- [20] G. Clifford Carter. Coherence and time delay estimation. *Proceedings of the IEEE*, 75(2):236–255, Feb 1987.
- [21] Koji Usami, Yoshihiro Nambu, Bao-Sen Shi, Akihisa Tomita, and Kazuo Nakamura. Observation of antinormally ordered hanbury brown-twiss correlations. *Phys. Rev. Lett.*, 92:113601, Mar 2004.
- [22] Joseph C. Hassab and R. Boucher. Optimum estimation of time delay by a generalized correlator. *Acoustics, Speech and Signal Processing, IEEE Transactions on*, 27(4):373–380, Aug 1979.
- [23] D Stucki, N Gisin, O Guinnard, G Ribordy, and H Zbinden. Quantum key distribution over 67 km with a plugplay system. *New Journal of Physics*, 4(1):41, 2002.
- [24] R. Ursin, F. Tiefenbacher, T. Schmitt-Manderbach, H. Weier, T. Scheidl, M. Lindenthal, B. Blauensteiner, T. Jennewein, J. Perdigues, P. Trojek, B. Omer, M. Furst, M. Meyenburg, J. Rarity, Z. Sodnik, C. Barbieri, H. Weinfurter, and A. Zeilinger. Entanglement-based quantum communication over 144 km. *Nat Phys*, 3(7):481–486, Jul 2007.
- [25] Alessandro Fedrizzi, Rupert Ursin, Thomas Herbst, Matteo Nespola, Robert Prevedel, Thomas Scheidl, Felix Tiefenbacher, Thomas Jennewein, and Anton Zeilinger. High-fidelity transmission of entanglement over a high-loss free-space channel. *Nat Phys*, 5(6):389–392, Jun 2009.